

Task-Space Position and Containment Control of Redundant Manipulators with Bounded Inputs

Amir Zakerimanesh¹, Ali Torabi², Farzad Hashemzadeh¹ and Mahdi Tavakoli²

Abstract—This note presents a novel approach for task-space tracking control of redundant manipulators with bounded actuation. Inspired by the leader-follower containment problem in multi-agent systems, the proposed controller is utilized to address the containment control of a single follower manipulator led by multiple manipulators. In the controller design, the redundancy of the robots is exploited for achieving sub-task control such as singularity avoidance, and joint limit avoidance. The asymptotic stability condition for the closed-loop dynamics is obtained using Lyapunov functional. For the containment, the proposed controller makes sure that the leaders track their desired positions and the follower robot's end-effector asymptotically converges to the convex hull formed by the leaders' traversed trajectories. The efficiency of the proposed control algorithm is verified through numerical simulations and experimental results.

I. INTRODUCTION

The control of multi-agent systems has caught on quickly due to its growing applicability in areas like autonomous vehicles, swarm robotics, and multilateral teleoperation [1]. In the area of the multi-agent system, the consensus problem in the presence of a leader and a follower is called the leader-follower consensus. With multiple leaders, the containment control emerges wherein the followers are to be steered into a given geometric shape spanned by the leaders [2]. The bottom line in the containment control is that the desired area should ultimately contain the system (e.g., a group of autonomous vehicles or robots). In practice, actuators can supply bounded signals, and thus the control torques are always subject to bounded actuation. This limitation can adversely affect the system's performance and render undesirable responses [3]. Therefore, addressing this limitation has practical importance and should be taken into account in the controller design.

In literature, various schemes have been proposed to address the stability and position tracking of the single manipulators subjected to saturation. In [4], a nonlinear anti-windup scheme has been proposed to guarantee stability and task-space tracking performance on Euler–Lagrange systems subject to input magnitude saturation. In [5], a nonlinear

PID regulator has been proposed to address the joint-space tracking and stability performance for manipulators with bounded torques. In [6], a robust adaptive model reference impedance controller is developed for an n-link robotic manipulator with parameter uncertainties, actuator saturation and imprecise force sensor measurement.

In teleoperation systems, the saturation compensation has been also received a great deal of attention. In [7], a nonlinear-proportional-derivative-like controller is designed under no velocity measurements for nonlinear teleoperation system in the presence of asymmetric time-varying delays and actuator saturation to address stability and joint-space tracking problems. The work in [8] introduces the nP+D controller by which addresses the stability and joint-space synchronization problem of the bilateral teleoperation system subject to actuator saturation and time-varying delays. In [9], an adaptive switching-based control framework is developed for joint-space synchronization problem of nonlinear teleoperation system with taking account of actuator saturation and asymmetric time-varying delays. In [10], to address the finite-time joint-space tracking control problem for nonlinear teleoperation systems, the anti-windup control framework is adopted and a modified anti-windup compensator is developed to analyze and handle the actuator saturation. In [11], an adaptive nonlinear fractional power proportional+damping control scheme is designed to address the joint-space synchronization control problem of flexible telerobotics with input saturation.

A kinematically redundant robot can be controlled in such a way as the joint motions do not affect the position of the end-effector [12]. This redundancy can be exploited to achieve a sub-task such as singularity avoidance, manipulability enhancement, and/or joint limit avoidance [13], [14] while performing the main task. In [15], a study has been done to show that the redundancy can be used to increase the manipulability of the human interface, and consequently improve the resolution of force feedback for the user. In the presence of actuators saturation, the proposed controller in [16] tackles the task-space position synchronization problem for bilateral teleoperation with the redundant remote robot. Our work exploits some overlooked properties of the nonlinear function introduced in [8] and proposes a novel controller along the lines of the controller of [16]. The main function of the proposed controller is to ensure that the stability and tracking performance of the single manipulator with bounded actuation is achieved. However, inspired by the containment problem in multi-agent systems [17], [18], and given that the desired reference trajectory for the follower

* This research was supported in part by the Canada Foundation for Innovation under Grant LOF 28241, in part by the Alberta Innovation and Advanced Education Ministry through Small Equipment under Grant RCP-12-021, in part by the Natural Science and Engineering Research Council of Canada through the Collaborative Health Research Projects, and in part by the Quanser, Inc.

¹Amir Zakerimanesh and Farzad Hashemzadeh are with the Faculty of Electrical and Computer Engineering, University of Tabriz, Tabriz, Iran. hashemzadeh@tabrizu.ac.ir

²Ali Torabi and Mahdi Tavakoli are with the Department of Electrical and Computer Engineering, University of Alberta, Edmonton, Alberta, Canada. ali.torabi@ualberta.ca and mahdi.tavakoli@ualberta.ca

in cooperating systems is typically determined by either the leaders' dynamics or preset time-varying functions, we have developed the problem formulation in such a way as to make the controller well-suited for the containment control of the redundant manipulator. The containment control is mainly utilized to ensure that a group of agents does not enter into unintended areas. In this case, a portion of agents as followers move into the region spanned by the leaders. Also, in the case of the proposed controller, it can force the robot to contain within the desired trajectories and so keeps the robot away from being diverted to the undesired paths during its move. Also, as another practical application of the containment control, the proposed method can enable a manipulator (e.g., a welding manipulator) to track not only predetermined trajectories but also the trajectories contained between them without the need for knowing their exact equation.

This paper is organized in sections as follows. Sections II and III give problem formulation and preliminaries while proposed controller and stability analysis are studied in Sections IV and V. In Section VI sub-task control and in Section VII simulation and experimental results are discussed. In Sections VIII and IX, conclusion and appendix are presented, respectively.

II. PROBLEM FORMULATION

In this section, we tend to formulate the problem of addressing both 1) tracking performance of the leader manipulators, each given a desired task-space trajectory. 2) the containment control in the task-space for the follower manipulator. We will briefly touch on the definition of the containment control in Section III. Let $\{\mathcal{L}_1, \mathcal{L}_2, \dots, \mathcal{L}_n\}$ denote the leader manipulators and n is the numbers of the leaders. Also, let \mathcal{F} be the follower. With the assumption that the redundant manipulators, either the leaders or the follower, are modeled by lagrangian systems, driven by actuated revolute joints and their control signals are subject to actuators saturation, let their dynamics be given by

$$M_k(q_k)\ddot{q}_k + C_k(q_k, \dot{q}_k)\dot{q}_k + G_k(q_k) = S_k(\tau_k) \quad (1)$$

where for $k \in \{\mathcal{L}_1, \mathcal{L}_2, \dots, \mathcal{L}_n, \mathcal{F}\}$, $q_k, \dot{q}_k, \ddot{q}_k \in \mathbb{R}^{\beta_k \times 1}$ are the vectors of the joints positions, velocities and accelerations of the robots, respectively, such that β_k denotes the number of joints. Also, $M_k(q_k) \in \mathbb{R}^{\beta_k \times \beta_k}$, $C_k(q_k, \dot{q}_k) \in \mathbb{R}^{\beta_k \times \beta_k}$ and $G_k(q_k) \in \mathbb{R}^{\beta_k \times 1}$ are the inertia matrix, the Coriolis/centrifugal matrix and the gravitational vector, respectively. The saturation of the control signals is modeled by the vector function $S_k(\tau_k): \mathbb{R}^{\beta_k \times 1} \rightarrow \mathbb{R}^{\beta_k \times 1}$ whose elements; $s_{k_i}(\tau_{k_i}): \mathbb{R} \rightarrow \mathbb{R}$, $i = 1, \dots, \beta_k$, are defined as follows

$$s_{k_i}(\tau_{k_i}) = \begin{cases} B_{k_i} & \text{if } \tau_{k_i} > B_{k_i} \\ \tau_{k_i} & \text{if } |\tau_{k_i}| \leq B_{k_i} \\ -B_{k_i} & \text{if } \tau_{k_i} < -B_{k_i} \end{cases} \quad (2)$$

where $B_{k_i} \in \mathbb{R}_{>0}$ is the saturation level of the corresponding actuator and τ_{k_i} denotes the control signal applied on the i^{th} joint of the relevant robot. It is imperative to have $0 < \Omega_{k_i} < B_{k_i}$ where $|g_{k_i}(q_k)| \leq \Omega_{k_i}$, and $g_{k_i}(q_k)$ is the i^{th} element of the gravity vector $G_k(q_k)$. This condition implies that the

actuators of the manipulators are capable of overcoming the gravity within their workspaces. Let $X_k \in \mathbb{R}^{\epsilon \times 1}$ represent the position of the robots in the task-space and ϵ denotes the dimension of the task-space. The relation between the task-space positions and the joint-space positions of the robots are as

$$X_k = h_k(q_k), \quad \dot{X}_k = J_k(q_k)\dot{q}_k \quad (3)$$

where $h_k(q_k): \mathbb{R}^{\beta_k \times 1} \rightarrow \mathbb{R}^{\epsilon \times 1}$ describes the nonlinear mapping between the joint-space positions and the task-space positions, and $J_k(q_k) \in \mathbb{R}^{\epsilon \times \beta_k}$ is the Jacobian matrix defined as $J_k(q_k) = \frac{\partial h_k(q_k)}{\partial q_k}$. For simplicity, in the rest of the paper notations M_k , C_k , G_k , J_k , J_k^T and J_k^+ are used instead of $M_k(q_k)$, $C_k(q_k, \dot{q}_k)$, $G_k(q_k)$, $J_k(q_k)$, $J_k^T(q_k)$ and $J_k^+(q_k)$ ($\mathbb{R}^{\beta_k \times 1} \rightarrow \mathbb{R}^{\beta_k \times \epsilon}$, being the pseudo-inverse of $J_k(q_k)$ defined later), respectively.

III. PRELIMINARIES

According to [19], [20], the important properties of the revolute-joint manipulators (1) are revisited as follows.

Property 1: The inertia matrix $M_k \in \mathbb{R}^{\beta_k \times \beta_k}$ is symmetric positive-definite and has the following upper and lower bounds as $0 < \lambda_{\min}(M_k)\mathbb{I}_{\beta_k} \leq M_k \leq \lambda_{\max}(M_k)\mathbb{I}_{\beta_k} < \infty$ where \mathbb{I}_{β_k} is the identity matrix of size β_k .

Property 2: $\dot{M}_k - 2C_k$ is a skew symmetric matrix.

Property 3: The gravity vector G_k is bounded. In other words, there exist positive constants Ω_{k_i} such that each element of the gravity vector g_{k_i} satisfies $|g_{k_i}| \leq \Omega_{k_i}$.

Property 4: For a manipulator with revolute joints, there exists a positive v bounding the Coriolis/centrifugal term as $\|C_k(q_k, x)y\|_2 \leq v\|x\|_2\|y\|_2$

A. Containment Control

Definition 1: The convex hull $Co(\mathbb{S})$ of a finite set of points $\mathbb{S} = \{s_1, s_2, \dots, s_n\}$ is the minimal convex set containing all points in \mathbb{S} . Expressing this as a single formula, the convex hull is the set [21]:

$$Co(\mathbb{S}) = \left\{ \sum_{z=1}^n a_z s_z \mid s_z \in \mathbb{S}, a_z \in \mathbb{R}, a_z \geq 0, \sum_{z=1}^n a_z = 1 \right\} \quad (4)$$

Consider the robots dynamics as (1). Let $X_{d_z}(t) \in \mathbb{R}^{\epsilon \times 1}$, $z = 1, \dots, n$, represent the desired task-space positions for the leader manipulators. Let the coefficient a_z be assigned to the z^{th} leader manipulator where for each choice of coefficients, the resulting convex combination is a point in the convex hull, and the whole convex hull can be formed by choosing coefficients in all possible ways. Also, let the leaders' task-space positions be as a set $\mathbb{C} \triangleq \{X_{\mathcal{L}_1}(t), \dots, X_{\mathcal{L}_n}(t)\}$. The error signal is defined as

$$e_k \triangleq \begin{cases} X_{\mathcal{L}_z}(t) - X_{d_z}(t) & \text{if } k = \mathcal{L}_z \\ X_{\mathcal{F}}(t) - Co(\mathbb{C}) & \text{if } k = \mathcal{F} \end{cases} \quad (5)$$

in which $e_{\mathcal{L}_z}$ and $e_{\mathcal{F}}$ denote task-space tracking error of the z^{th} leader manipulator and the containment error of the follower, respectively. Also, $X_{d_z}(t)$ shows the desired task-space position for the z^{th} leader. Furthermore, it is assumed that the given desired positions have bounded and continuous first and second derivatives.

It is worth noting that various selection of the coefficients a_z can be used as the dominance factors in the shared autonomy teleoperation systems in which one leader is controlled by a human user and the other leaders are prompted by the computer-generated commands, and the controlled interplay of the coefficients will determine which direction of action the follower robot (slave) takes.

Definition 2: The follower robot achieves containment if the control law ensures that its task-space position will converge to the convex hull formed by the leaders' task-space positions as $t \rightarrow \infty$. In other words, $e_{\mathcal{F}} \rightarrow 0$.

B. Incorporation of sub-task control into the controller

To lay the groundwork for achieving the containment control and a sub-task control, inspired by [13], [22], let us find the modified form of the robots' dynamics in order to incorporate the sub-task control into the controllers development. To achieve this, let signals $\zeta_k \in \mathbb{R}^{\beta_k \times 1}$ and $\varphi_k \in \mathbb{R}^{\beta_k \times 1}$ be defined as $\varphi_k \triangleq \dot{q}_k - \zeta_k$ and

$$\zeta_k \triangleq \begin{cases} J_{\mathcal{L}_z}^+ \left(-e_{\mathcal{L}_z} + \dot{X}_{d_z} \right) + (\mathbb{I}_{\beta_k} - J_{\mathcal{L}_z}^+ J_{\mathcal{L}_z}) \Psi_{\mathcal{L}_z} & \text{if } k = \mathcal{L}_z \\ J_{\mathcal{F}}^+ \left(-e_{\mathcal{F}} + \sum_{z=1}^n \dot{X}_{\mathcal{L}_z} \right) + (\mathbb{I}_{\beta_k} - J_{\mathcal{F}}^+ J_{\mathcal{F}}) \Psi_{\mathcal{F}} & \text{if } k = \mathcal{F} \end{cases} \quad (6)$$

where $\Psi_k \in \mathbb{R}^{\beta_k \times 1}$ is the negative gradient of an appropriately defined function for the sub-task control. Also, $J_k^+ \in \mathbb{R}^{\beta_k \times \epsilon}$ is the pseudo-inverse of J_k defined by $J_k^+ \triangleq J_k^T (J_k J_k^T)^{-1}$ which satisfies $J_k J_k^+ = \mathbb{I}_{\beta_k}$ and $J_k (\mathbb{I}_{\beta_k} - J_k^+ J_k) = 0$, and accordingly $J_k (\mathbb{I}_{\beta_k} - J_k^+ J_k) \Psi_k = 0$ which in turn implies that $(\mathbb{I}_{\beta_k} - J_k^+ J_k)$ projects the vector Ψ_k onto the null space of J_k . Therefore, if the link velocity in the null space of J_k is such that tracks $(\mathbb{I}_{\beta_k} - J_k^+ J_k) \Psi_k$, then not only it will not influence the task-space motion, but also it can be regulated by Ψ_k . Now, taking the derivative of the both sides of the equation $\varphi_k = \dot{q}_k - \zeta_k$ with respect to time, premultiplying them by the inertia matrix M_k and substituting $M_k \ddot{q}_k$ with its equivalent from (1), the robot's modified dynamics can be derived as

$$M_k \dot{\varphi}_k + C_k \varphi_k = \Theta_k + S_k(\tau_k); \quad \Theta_k \triangleq M_k \dot{\zeta}_k + C_k \zeta_k - G_k \quad (7)$$

IV. PROPOSED CONTROLLER

In this part, the proposed controller is intended for achieving $e_k \rightarrow 0$. Consider the dynamical system (7) and let the control signal be given by

$$\tau_k = -\underbrace{\Theta_k - J_k^T \left(\frac{\partial P_k(e_k)}{\partial e_k} \Phi_k P_k(e_k) + \Lambda_k \dot{e}_k \right)}_{\triangleq \Delta_k} - \Sigma_k \varphi_k \quad (8)$$

where $\Phi_k, \Lambda_k \in \mathbb{R}^{\epsilon \times \epsilon}$ and $\Sigma_k \in \mathbb{R}^{\beta_k \times \beta_k}$ are positive-definite diagonal matrices with elements $\phi_{k_j} \in \mathbb{R}_{>0}$, $\lambda_{k_j} \in \mathbb{R}_{>0}$ and $\sigma_{k_i} \in \mathbb{R}_{>0}$, respectively. Motivated by [8], for any $x_{k_j} \in \mathbb{R}$ and $X_k \in \mathbb{R}^{\epsilon \times 1}$, $P_k(X_k): \mathbb{R}^{\epsilon \times 1} \rightarrow \mathbb{R}^{\epsilon \times 1}$ is a nonlinear vector function with elements $p_{k_j}(x_{k_j}): \mathbb{R} \rightarrow \mathbb{R}$; $j=1, \dots, \epsilon$. The nonlinear scalar function $p_{k_j}(x_{k_j})$ is required to be strictly increasing, bounded, continuous, passing through the origin, concave for positive x_{k_j} and convex for negative x_{k_j} with continuous first and second derivative around the origin such that $|p_{k_j}(x_{k_j})| \leq |x_{k_j}|$, $p_{k_j}(-x_{k_j}) = -p_{k_j}(x_{k_j})$, $0 \leq p_{k_j}(x_{k_j}) p_{k_j}(x_{k_j}) \leq x_{k_j} p_{k_j}(x_{k_j}) \leq x_{k_j} x_{k_j}$ and

$\frac{\partial P_k(X_k)}{\partial X_k} \leq \text{diag}\{\varpi_{k_1}, \dots, \varpi_{k_\epsilon}\}$ where $0 < \frac{\partial p_{k_j}(x_{k_j})}{\partial x_{k_j}} \leq \varpi_{k_j}$. For instance, by choosing $p_{k_j}(x_{k_j}) = b_{k_j} \tan^{-1}(x_{k_j})$; $0 < b_{k_j} \leq 1$, all the mentioned properties are satisfied, $\frac{\partial p_{k_j}(x_{k_j})}{\partial x_{k_j}}$ is positive and bounded such that $\xi_k \triangleq \frac{\partial P_k(X_k)}{\partial X_k} \leq \text{diag}\{b_{k_1}, \dots, b_{k_\epsilon}\} \leq \mathbb{I}_\epsilon$ and $N_{k_j} \triangleq \sup p_{k_j}(x_{k_j}) = b_{k_j} \pi/2$. Note that $\text{diag}\{b_{k_1}, \dots, b_{k_\epsilon}\}$ denotes a block-diagonal matrix formed by $b_{k_1}, b_{k_2}, \dots, b_{k_n}$.

V. STABILITY ANALYSIS

In this section, the stability and asymptotic performance of the system (7) with the proposed controller (8) is analyzed. Applying the controller to the modified dynamics, the following closed-loop dynamics can be found:

$$M_k \dot{\varphi}_k + C_k \varphi_k = S_k(\Delta_k - \Sigma_k \varphi_k) + \Theta_k \quad (9)$$

Theorem 1: Assume that $\dot{X}_{d_z}, \ddot{X}_{d_z} \in L_\infty$ and the robots (7) are able to avoid the singularities. With the proposed controller (8), the leaders converge asymptotically to the desired task-space positions, and the follower robot achieves the containment regardless of whether $\Psi_k = 0$ or $\Psi_k \neq 0$, provided that

$$\phi_{k_{max}} < \frac{B_{k_{min}} - \Omega_{k_{max}} - \Upsilon_k}{\epsilon \varpi_{k_{max}} J_{k_{max}} N_{k_{max}}} \quad (10)$$

where $\Upsilon_k \triangleq \max_i \left\{ \sum_{b=1}^{\beta_k} \left(M_{k_{ib}} \dot{\zeta}_{k_b} + C_{k_{ib}} \zeta_{k_b} \right) + \sum_{j=1}^{\epsilon} J_{k_{ji}} \lambda_{k_j} \dot{e}_{k_j} \right\}$, $\varpi_{k_{max}} \triangleq \max_j \{\varpi_{k_j}\}$, $\phi_{k_{max}} \triangleq \max_j \{\phi_{k_j}\}$, $N_{k_{max}} \triangleq \max_j \{N_{k_j}\}$, $B_{k_{min}} \triangleq \min_i \{B_{k_i}\}$ and $\Omega_{k_{max}} \triangleq \max_i \{\Omega_{k_i}\}$. Also, $M_{k_{ib}}, C_{k_{ib}} \in \mathbb{R}$ are the elements of M_k and C_k matrices, respectively in which $i, b = 1, \dots, \beta_k$. Moreover, $\zeta_{k_b}, \dot{\zeta}_{k_b} \in \mathbb{R}$ are the elements of the vectors ζ_k and $\dot{\zeta}_k$, respectively. Also, $J_{k_{max}} \triangleq \max_{j,i} \{\sup |J_{k_{ji}}|\}$. Note that $J_{k_{ji}}$ are the elements of the matrix J_k such that $j = 1, \dots, \epsilon$ and $i = 1, \dots, \beta_k$.

Proof: Consider the positive definite storage function

$$V(t) = \frac{1}{2} \sum_k \left(\varphi_k^T M_k \varphi_k + P_k^T(e_k) \Phi_k P_k(e_k) + e_k^T \Lambda_k e_k + 2 \int_0^t \sum_{i=1}^{\beta_k} -\varphi_{k_i}(\mu) (s_{k_i}(\Delta_{k_i}(\mu)) - \sigma_{k_i} \varphi_{k_i}(\mu)) - \Delta_{k_i}(\mu) d\mu \right) \quad (11)$$

where $\Delta_{k_i}(\mu)$; the elements of $\Delta_k(\mu)$, can be shown as

$$\triangleq -\theta_{k_i}(\mu) - \sum_{j=1}^{\epsilon} J_{k_{ji}} \left(\frac{\partial p_{k_j}(e_{k_j}(\mu))}{\partial e_{k_j}(\mu)} \phi_{k_j} p_{k_j}(e_{k_j}(\mu)) + \lambda_{k_j} \dot{e}_{k_j}(\mu) \right) \quad (12)$$

such that (see APPENDIX)

$$-\varphi_{k_i}(\mu) (s_{k_i}(\Delta_{k_i}(\mu)) - \sigma_{k_i} \varphi_{k_i}(\mu)) - \Delta_{k_i}(\mu) \geq 0 \quad (13)$$

Note that $\theta_{k_i}(\mu) \in \mathbb{R}$ denotes the elements of the vector $\Theta_k(\mu) \in \mathbb{R}^{\beta_k \times 1}$. Now, given (9) and Property 2, differentiating the storage function $V(t)$ along the system trajectory results in

$$\dot{V}(t) = \sum_k \left(\varphi_k^T (S_k(\Delta_k - \Sigma_k \varphi_k) + \Theta_k) + P_k^T(e_k) \Phi_k \frac{\partial P_k(e_k)}{\partial e_k} \dot{e}_k + e_k^T \Lambda_k \dot{e}_k - \varphi_k^T (S_k(\Delta_k - \Sigma_k \varphi_k) - \Delta_k) \right) \quad (14)$$

Therefore, considering the fact that $J_k \varphi_k = e_k + \dot{e}_k$ yields

$$\begin{aligned} \dot{V}(t) &= \sum_k \left(-\varphi_k^T J_k^T \frac{\partial P_k(e_k)}{\partial e_k} \Phi_k P_k(e_k) - \varphi_k^T J_k^T \Lambda_k \dot{e}_k \right. \\ &\quad \left. + P_k^T(e_k) \Phi_k \frac{\partial P_k(e_k)}{\partial e_k} \dot{e}_k + e_k^T \Lambda_k \dot{e}_k \right) \\ &= \sum_k \left(-e_k^T \frac{\partial P_k(e_k)}{\partial e_k} \Phi_k P_k(e_k) - \dot{e}_k^T \Lambda_k \dot{e}_k \right) \\ &\leq \sum_k \left(-P_k^T(e_k) \xi_k \Phi_k P_k(e_k) - \dot{e}_k^T \Lambda_k \dot{e}_k \right) \end{aligned} \quad (15)$$

In conclusion, we would have $\dot{V}(t) \leq 0$, which means all terms in $V(t)$ are bounded. Therefore, $\varphi_k, P_k(e_k), e_k \in L_\infty$ and given $J_k \varphi_k = e_k + \dot{e}_k$ results in $\dot{e}_k \in L_\infty$ and so $\frac{d}{dt}(P_k(e_k)) \in L_\infty$. Given $\dot{X}_{d_z} \in L_\infty$ and $\dot{e}_k \in L_\infty$ yields $\dot{X}_k \in L_\infty$. Integrating both sides of (15), it is possible to see that $P_k(e_k), \dot{e}_k \in L_2$. Given $\dot{X}_k \in L_\infty$ results in $\dot{q}_k \in L_\infty$. Given the system dynamics (1), $\dot{q}_k \in L_\infty$, and Properties 1, 3 and 4 results in $\ddot{q}_k \in L_\infty$, and considering $\ddot{X}_k = J_k \ddot{q}_k + \dot{J}_k \dot{q}_k$ stands to reason that $\ddot{X}_k \in L_\infty$. Also, $\ddot{X}_{d_z}, \ddot{X}_k \in L_\infty$ readily leads to $\ddot{e}_k \in L_\infty$. Because $\ddot{e}_k, \frac{d}{dt}(P_k(e_k)) \in L_\infty$ and $\dot{e}_k, P_k(e_k) \in L_2$, using Barbalat's lemma results in $\dot{e}_k, P_k(e_k) \rightarrow 0$. Noting that for any $x_{k_j} \in \mathbb{R}$, $p_{k_j}(x_{k_j})$ passes through the origin, we get $e_k \rightarrow 0$. Therefore, the containment is achieved and the proof of Theorem 1 is completed. Having shown that $e_k, \dot{e}_k \rightarrow 0$, and assuming that the robots are able to avoid the singularities, results in $\varphi_k \rightarrow 0$. It is worth noting that by the containment achievement the follower manipulator converges to a "scaled" centroid of the convex hull defined by the leaders wherein the parameter a_z plays the role of dominance factor (mainly used in the shared control systems) of the z^{th} leader manipulator. ■

Remark 1: In stability condition (10), the parameters $\Omega_{k_{max}}$ and $J_{k_{max}}$ are function of the robots' physical parameters. Therefore, disparities between real (let be denoted by an overbar notation) and nominal values affect the system's stability. For the sake of simplicity, let's assume that the sub-task control is not required. Thus, the stability condition becomes

$$\phi_{k_{max}} < \frac{B_{k_{min}} - \Omega_{k_{max}}}{\epsilon \varpi_{k_{max}} J_{k_{max}} N_{k_{max}}}$$

If nominal values are bigger than real values, then we get $\Omega_{k_{max}} > \bar{\Omega}_{k_{max}}$ and $J_{k_{max}} > \bar{J}_{k_{max}}$ which consequently results in

$$\phi_{k_{max}} < \frac{B_{k_{min}} - \Omega_{k_{max}}}{\epsilon \varpi_{k_{max}} J_{k_{max}} N_{k_{max}}} \implies \phi_{k_{max}} < \frac{B_{k_{min}} - \bar{\Omega}_{k_{max}}}{\epsilon \varpi_{k_{max}} \bar{J}_{k_{max}} N_{k_{max}}}$$

Also, if nominal values are lesser than real values, then we get $\Omega_{k_{max}} < \bar{\Omega}_{k_{max}}$ and $J_{k_{max}} < \bar{J}_{k_{max}}$ which consequently results in

$$\phi_{k_{max}} < \frac{B_{k_{min}} - \Omega_{k_{max}}}{\epsilon \varpi_{k_{max}} J_{k_{max}} N_{k_{max}}} \not\Rightarrow \phi_{k_{max}} < \frac{B_{k_{min}} - \bar{\Omega}_{k_{max}}}{\epsilon \varpi_{k_{max}} \bar{J}_{k_{max}} N_{k_{max}}}$$

Therefore, using the nominal values, we should set the controller parameters far enough beyond the stability condition's boundary in order to keep the system stable.

VI. SUB-TASK CONTROL

This section adopts a similar approach used in [13] for the sub-task control of the redundant robots. As mentioned

earlier, the link velocity in the null space of J_k does not influence the task-space motion and does not contribute to the task-space velocity. Therefore, if it is such that tracks $[\mathbb{I}_{\beta_k} - J_k^+ J_k] \Psi_k$, then the movement of the telemanipulator in this configuration-dependent subspace can be regulated by Ψ_k . This kind of motion is called self-motion since it is not observed at the end-effector [12]. The function $[\mathbb{I}_{\beta_k} - J_k^+ J_k] \Psi_k$ can be considered as the desired velocity in the null space of J_k through which one can define an appropriate function for Ψ_k to complete the sub-task control. On the one hand, the sub-task tracking error for the redundant robot (let it be $e_{k_{ste}}$) was defined as $e_{k_{ste}} \triangleq [\mathbb{I}_{\beta_k} - J_k^+ J_k] (\dot{q}_k - \Psi_k)$ [12] where, on the other hand, it can be shown as well as

$$e_{k_{ste}} \triangleq [\mathbb{I}_{\beta_k} - J_k^+ J_k] (\dot{q}_k - \Psi_k) = [\mathbb{I}_{\beta_k} - J_k^+ J_k] \varphi_k \quad (16)$$

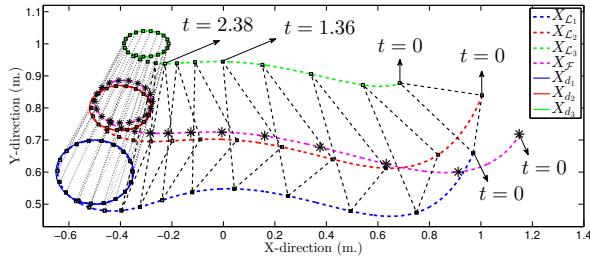
in which the properties $[\mathbb{I}_{\beta_k} - J_k^+ J_k] [\mathbb{I}_{\beta_k} - J_k^+ J_k] = \mathbb{I}_{\beta_k} - J_k^+ J_k$ and $[\mathbb{I}_{\beta_k} - J_k^+ J_k] J_k^+ = 0$ are used [12]. Therefore, if $\varphi_k \rightarrow 0$ (Theorem 1), then the sub-task tracking error approaches the origin and the link velocity in the null space of J_k tracks $[\mathbb{I}_{\beta_k} - J_k^+ J_k] \Psi_k$. The gradient projection method [23] is utilized in this paper to achieve the sub-task control. As described in [13], the sub-task of the robot can be controlled by any differentiable auxiliary function Ψ_k provided that it is expressed in terms of the joint angles or the end-effector position. Hence, one can define a differentiable cost function $f(q_k): \mathbb{R}^{\beta_k \times 1} \rightarrow \mathbb{R}$ for which a lower value corresponds to more desirable configurations. Then, the auxiliary function $\Psi_k = -\frac{\partial}{\partial q_k} f(q_k)$ can be utilized for achieving the sub-task control of the robot.

VII. SIMULATION AND EXPERIMENTAL RESULTS

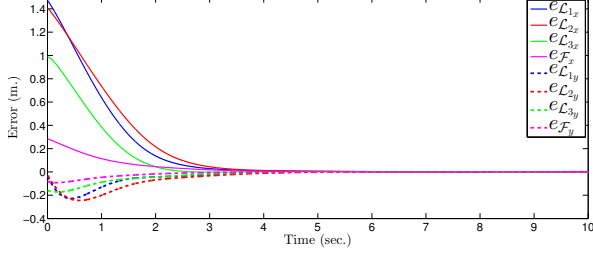
In this section, verification of results is provided through simulation and experimental conducts. In both the simulations and experiments, we have three robots as the leaders and one robot as the follower. Using the proposed controller, each leader tracks its desired task-space position and the follower converges to the convex hull formed by the leaders' task-space trajectories.

A. Simulation results

For simulations, the manipulators all are assumed to be 3-DoF planar revolute-joint robots. The links lengths for the first leader, the second leader, the third leader and the follower are $[0.4, 0.4, 0.4] m$, $[0.45, 0.45, 0.45] m$, $[0.42, 0.42, 0.42] m$ and $[0.5, 0.5, 0.5] m$, respectively. The links masses in the same order are $[0.35, 0.35, 0.35] kg$, $[0.4, 0.4, 0.4] kg$, $[0.37, 0.37, 0.37] kg$ and $[0.42, 0.42, 0.42] kg$. The conditions $q_{L_1}(0) = [\frac{\pi}{7}, \frac{\pi}{7}, -\frac{\pi}{7}]^T$, $q_{L_2}(0) = [\frac{\pi}{6}, \frac{\pi}{6}, -\frac{\pi}{6}]^T$, $q_{L_3}(0) = [\frac{\pi}{8}, \frac{\pi}{8}, \frac{\pi}{4}]^T$ and $q_F(0) = [\frac{\pi}{8}, \frac{\pi}{4}, -\frac{\pi}{3}]^T$ are chosen for the robots' initial joints positions. Also, it is assumed that $\dot{q}_k(0) = \ddot{q}_k(0) = 0$. The nonlinear function $p_{k_j}(x_{k_j}) = \tan^{-1}(x_{k_j})$ is used in the controllers, i.e., $N_{k_j} = N_{k_{max}} = \frac{\pi}{2}$ and $\varpi_{k_j} = \varpi_{k_{max}} = 1$. It is assumed that the control signals are subject to the actuators saturation at levels $+20 N/m$ and $-20 N/m$ which means $B_{k_i} = B_{k_{min}} = 20 N/m$. Also, in the controller (8), the matrices Λ_k and Σ_k are assumed to be the identity matrixes of sizes 2 and 3, respectively.



(a) The traversed trajectories and the containment achievement.



(b) The convergence of the error signals to zero.

Fig. 1: The task-space positions and the error signals.

Having clues from [12], [22], for the singularity avoidance, the auxiliary function is assumed to be $\Psi_k \triangleq -0.01(q_{k1} - 2q_{k2} + q_{k3})[1, -2, 1]^T$ which is the negative of the gradient of the cost function $f(q_k) = 0.005(q_{k3} - 2q_{k2} + q_{k1})^2$. Let the desired task-space positions for the leaders be given as

$$\begin{cases} X_{d1} = [-0.5 + 0.15\sin(t) \quad 0.6 + 0.1\cos(t)]^T \\ X_{d2} = [-0.4 + 0.12\sin(t) \quad 0.8 + 0.07\cos(t)]^T \\ X_{d3} = [-0.3 + 0.09\sin(t) \quad 1 + 0.04\cos(t)]^T \end{cases} \quad (17)$$

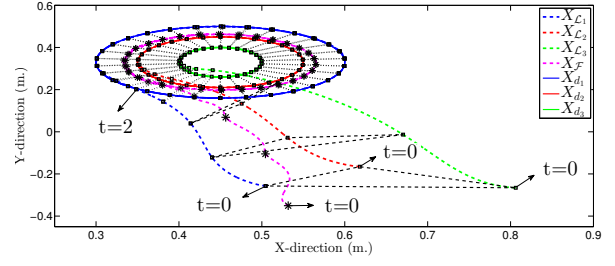
and for the containment control, let the coefficients be equal to $a_1 = 0.3$, $a_2 = 0.3$ and $a_3 = 0.4$. Therefore, for $k \in \{\mathcal{L}_1, \mathcal{L}_2, \mathcal{L}_3, \mathcal{F}\}$, the controllers are

$$\tau_k = -\Theta_k - J_k^T \left(\begin{bmatrix} \frac{\phi_{kmax}}{1 + e_{kx} e_{ky}} & 0 \\ 0 & \frac{\phi_{kmax}}{1 + e_{kx} e_{ky}} \end{bmatrix} P_k(e_k) + \dot{e}_k \right) - \varphi_k \quad (18)$$

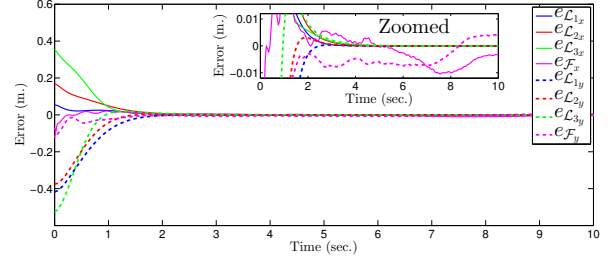
which are designed to have the leaders reach and track the desired positions (17), and render the follower robot's end-effector converged to the convex hull formed by the leaders' trajectories. Fig. 1 shows the leaders' desired task-space positions, the robots' trajectories in the task-space and the error signals. As we see in Fig. 1a, the leaders' end-effectors converge asymptotically to the desired task-space positions, and the follower's end-effector converges to the convex hull formed by the leaders' task-space positions. Please note that at any moment of the simulation, the smallest convex polygon containing the leaders' trajectories is a dashed line triangle formed by the leaders' trajectories as the triangle's vertices. Also, it is worth noting that at $t=0$ sec the follower's end-effector (designated by asterisks) is outside the triangle, but as the time elapses, it goes gradually inside the triangle. Also, Fig. 1b shows the error signals, in which the subscripts x and y denote the errors in the X and Y directions, respectively.

B. Experimental results

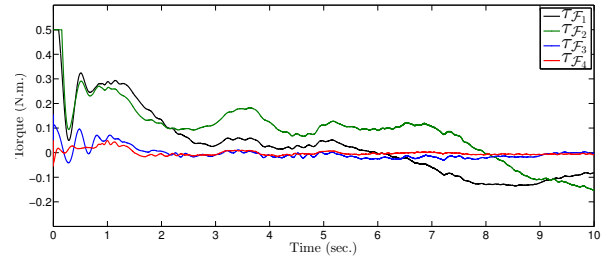
To provide evidence for the feasibility of the proposed controller in practice, three simulated 3-DoF planar revolute-joint robots are considered as the leaders (like the simulation



(a) Experiment results: The robots traversed trajectories.



(b) Experiment results: The convergence of the error signals to zero.



(c) Experiment results: Joints torque of the follower.

Fig. 2: The task-space positions and the error signals.

section), and one real 4-DoF planar robot is used as the follower which is developed by serially connecting two robots, a 2-DoF PHANToM 1.5A (Geomagic Inc., Morrisville, NC, USA) and a 2-DoF planar upper-limb rehabilitation robot 1.0 (Quanser Inc., Markham, ON, Canada). The base joint of the 3-DoF PHANToM robot is detached to turn it into a 2-DoF planar robot. The links lengths for the first leader, the second leader, the third leader and the follower are $[0.4, 0.4, 0.4]$ m, $[0.37, 0.37, 0.37]$ m, $[0.35, 0.35, 0.35]$ m and $[0.254, 0.140, 0.210, 0.170]$ m, respectively. The links masses in the same order for the leaders are $[0.35, 0.35, 0.35]$ kg, $[0.32, 0.32, 0.32]$ kg and $[0.3, 0.3, 0.3]$ kg. Also, initial joints positions for the robots are $q_{\mathcal{L}_1}(0) = [\frac{\pi}{4}, \frac{-2\pi}{5}, \frac{-2\pi}{5}]^T$, $q_{\mathcal{L}_2}(0) = [\frac{\pi}{4}, \frac{-\pi}{3}, \frac{-\pi}{3}]^T$, $q_{\mathcal{L}_3}(0) = [\frac{-\pi}{5}, \frac{\pi}{4}, \frac{-\pi}{5}]^T$ and $q_{\mathcal{F}}(0) = [0, 0, \frac{-\pi}{8}, \frac{\pi}{4}]^T$. The follower robot has joint angle limitation such that $q_{\mathcal{F}_1, min} = -0.95$ rad, $q_{\mathcal{F}_1, max} = 1.57$ rad, $q_{\mathcal{F}_2, min} = 0$ rad, $q_{\mathcal{F}_2, max} = 2.53$ rad, $q_{\mathcal{F}_3, min} = -0.95$ rad, $q_{\mathcal{F}_3, max} = 2$ rad, $q_{\mathcal{F}_4, min} = -0.34$ rad and $q_{\mathcal{F}_4, max} = 1.39$ rad. Therefore, to obtain the auxiliary function for the follower and maintain the joint limits, the following cost function [24] is used.

$$f(q_{\mathcal{F}}) \triangleq \frac{1}{2} \sum_{j=1}^4 \left(\frac{q_{\mathcal{F}_j} - q_{\mathcal{F}_j, mid}}{q_{\mathcal{F}_j, max} - q_{\mathcal{F}_j, min}} \right)^2 \quad (19)$$

The saturation levels for the real robot are set to be at $+0.5$ N/m and -0.5 N/m, i.e., $B_{\mathcal{F}_i} = B_{\mathcal{F}_i, min} = 0.5$ N/m. For the containment control, the coefficients are assumed to

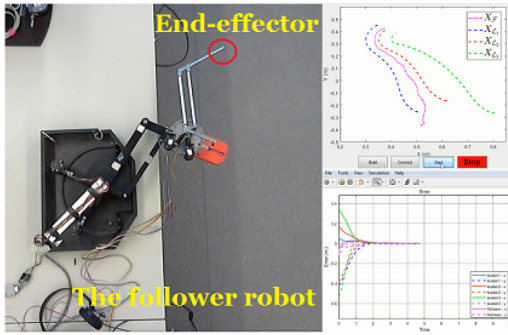


Fig. 3: A snapshot of the experiment on the 4-DoF robot.

be to $a_1=0.6$, $a_2=0.2$ and $a_3=0.2$. Also, in the controller (8) of the follower, the matrices $\Lambda_{\mathcal{F}}$ and $\Sigma_{\mathcal{F}}$ are assumed to be $\text{diag}(0.01,0.01)$ and $\text{diag}(0.015,0.015,0.015,0.015)$, respectively. Please note that given (15), Λ_k needs to be positive definite, and Σ_k is assumed to be positive definite and (13) is proved accordingly. The quasi-experimental results are shown in Fig. 2. The leaders are given concentric desired trajectories, and as Fig. 2a shows, the leaders' end-effectors reach and track the desired positions, and the follower reaches the containment which both are clear from Fig. 2b where shows the convergence of the error signals to zero. Also, it is worth noting that the robots' dynamics (1) are considered based on certain dynamics, and practical features like friction are ignored. Therefore, this may account for the noticeable swing of the follower's error signals near zero which is shown by the zoomed section in Fig. 2b. The joints' torque of the follower is depicted in Fig. 2c. As shown in this figure, the first and the second joints of the follower are saturated during the first 0.1 second of the experiment. Fig. 3 shows a snapshot of the experiment video¹ prepared to shed more light on the issue. The readers are strongly encouraged to download and watch the video.

VIII. CONCLUSION

In this note, a novel scheme was presented to address the task-space position control of redundant manipulators whose actuators practically supply bounded torques. The redundancy was incorporated into the controller development to achieve a sub-task control. The asymptotic stability of the closed-loop dynamics was studied using a Lyapunov functional under conditions on the controller parameters. It was shown that the controller is well-suited to the containment control of the redundant manipulator. The validity of the proposed controller was verified using numerical simulations and experimental results.

IX. APPENDIX

Proof of inequality (13): Following (2) and the condition (10), one can readily conclude that

$$|\Delta_{k_i}(\mu)| \leq B_{k_i} \quad \text{and} \quad \Delta_{k_i}(\mu) = s_{k_i}(\Delta_{k_i}(\mu)) \quad (\text{A.1})$$

Due to the strictly increasing property of the saturation function (2) in the linear region, we have

$$\begin{cases} s_{k_i}(\Delta_{k_i}(\mu)) \leq s_{k_i}(\Delta_{k_i}(\mu)) & \text{if } \varphi_{k_i}(\mu) \geq 0 \\ s_{k_i}(\Delta_{k_i}(\mu)) > s_{k_i}(\Delta_{k_i}(\mu)) & \text{if } \varphi_{k_i}(\mu) < 0 \end{cases} \quad (\text{A.2})$$

¹<https://bit.ly/2XXCzun>

Therefore, it can be concluded that

$$\varphi_{k_i}(\mu)(s_{k_i}(\Delta_{k_i}(\mu)) - \sigma_{k_i}\varphi_{k_i}(\mu)) - \Delta_{k_i}(\mu) \leq 0 \quad (\text{A.3})$$

REFERENCES

- [1] R. Olfati-Saber, J. A. Fax, and R. M. Murray, "Consensus and cooperation in networked multi-agent systems," *Proceedings of the IEEE*, vol. 95, no. 1, pp. 215–233, Jan 2007.
- [2] Z. Li, Z. Duan, W. Ren, and G. Feng, "Containment control of linear multi-agent systems with multiple leaders of bounded inputs using distributed continuous controllers," *International Journal of Robust and Nonlinear Control*, vol. 25, no. 13, pp. 2101–2121, 2015.
- [3] W. He, Y. Dong, and C. Sun, "Adaptive neural impedance control of a robotic manipulator with input saturation," *IEEE Trans. Syst., Man, Cybern.*, vol. 46, no. 3, pp. 334–344, 2016.
- [4] F. Morabito, A. R. Teel, and L. Zaccarian, "Nonlinear antiwindup applied to euler-lagrange systems," *IEEE Trans. Robot. Autom.*, vol. 20, no. 3, pp. 526–537, 2004.
- [5] V. Santibañez, K. Camarillo, J. Moreno-Valenzuela, and R. Campa, "A practical pid regulator with bounded torques for robot manipulators," *Int. J. Control. Autom. Syst.*, vol. 8, no. 3, pp. 544–555, 2010.
- [6] E. Arefinia, H. A. Talebi, and A. Doustmohammadi, "A robust adaptive model reference impedance control of a robotic manipulator with actuator saturation," *IEEE Trans. Syst., Man, Cybern.*, pp. 1–12, 2018.
- [7] D.-H. Zhai and Y. Xia, "Robust saturation-based control of bilateral teleoperation without velocity measurements," *Int. J. Robust Nonlinear Control*, vol. 25, no. 15, pp. 2582–2607, 2015.
- [8] F. Hashemzadeh, I. Hassanzadeh, and M. Tavakoli, "Teleoperation in the presence of varying time delays and sandwich linearity in actuators," *Automatica*, vol. 49, no. 9, pp. 2813–2821, 2013.
- [9] D.-H. Zhai and Y. Xia, "Adaptive control for teleoperation system with varying time delays and input saturation constraints," *IEEE Trans. Ind. Electron.*, vol. 63, no. 11, pp. 6921–6929, 2016.
- [10] D. Zhai and Y. Xia, "Finite-time control of teleoperation systems with input saturation and varying time delays," *IEEE Trans. Syst., Man, Cybern.*, vol. 47, no. 7, pp. 1522–1534, July 2017.
- [11] Y. Yang, J. Li, C. Hua, and X. Guan, "Adaptive synchronization control design for flexible telerobotics with actuator fault and input saturation," *Int. J. Robust Nonlinear Control*, vol. 28, no. 3, pp. 1016–1034, 2018.
- [12] P. Hsu, J. Mauser, and S. Sastry, "Dynamic control of redundant manipulators," *J. Field Robot.*, vol. 6, no. 2, pp. 133–148, 1989.
- [13] Y.-C. Liu *et al.*, "Control of semi-autonomous teleoperation system with time delays," *Automatica*, vol. 49, no. 6, pp. 1553–1565, 2013.
- [14] A. Zakerimanesh, F. Hashemzadeh, A. Torabi, and M. Tavakoli, "Controlled synchronization of nonlinear teleoperation in task-space with time-varying delays," *Int. J. Control. Autom. Syst.*, vol. 0, no. 0, pp. 1–9, 2019.
- [15] A. Torabi, M. Khadem, K. Zareinia, G. R. Sutherland, and M. Tavakoli, "Application of a redundant haptic interface in enhancing soft-tissue stiffness discrimination," *IEEE Robotics and Automation Letters*, vol. 4, no. 2, pp. 1037–1044, April 2019.
- [16] A. Zakerimanesh, F. Hashemzadeh, and M. Tavakoli, "Task-space synchronization of nonlinear teleoperation with time-varying delays and actuator saturation," *Int. J. Control*, vol. 0, no. 0, pp. 1–17, 2018.
- [17] H. Haghshenas, M. A. Badamchizadeh, and M. Baradarannia, "Containment control of heterogeneous linear multi-agent systems," *Automatica*, vol. 54, pp. 210–216, 2015.
- [18] J. R. Klotz, T.-H. Cheng, and W. E. Dixon, "Robust containment control in a leader-follower network of uncertain euler-lagrange systems," *International Journal of Robust and Nonlinear Control*, vol. 26, no. 17, pp. 3791–3805, 2016.
- [19] M. W. Spong, S. Hutchinson, and M. Vidyasagar, *Robot modeling and control*. Wiley New York, 2006, vol. 3.
- [20] R. Kelly, V. S. Davila, and J. A. L. Perez, *Control of robot manipulators in joint space*. Springer Science & Business Media, 2006.
- [21] R. T. Rockafellar, *Convex analysis*. Princeton university press, 2015.
- [22] E. Zergeroglu, D. D. Dawson, I. W. Walker, and P. Setlur, "Nonlinear tracking control of kinematically redundant robot manipulators," *IEEE/ASME Trans. Mechatronics*, vol. 9, no. 1, pp. 129–132, 2004.
- [23] B. Siciliano, "Kinematic control of redundant robot manipulators: A tutorial," *J. Intell. Robot. Syst.*, vol. 3, no. 3, pp. 201–212, 1990.
- [24] M. Ito, K. Kawatsu, and M. Shibata, "Kinematic control of redundant manipulators for admitting joint range of motion maximally," *IEEE Journal of Industry Applications*, vol. 6, no. 4, pp. 278–285, 2017.